ELSEVIER

Solid State Ionics 126 (1999) 227–234

SOLID STATE IONICS

www.elsevier.com/locate/ssi

Neutron diffraction study of electrochemically delithiated $LiMn_2O_4$ spinel

H. Berg*, J.O. Thomas

Inorganic Chemistry, Ångstrom Laboratory Uppsala University, Box 538, SE-751 21 Uppsala, Sweden

Received 2 July 1999; accepted 7 July 1999

Abstract

Partially electrochemically delithiated $LiMn_2O_4$ has been studied by a combination of in situ X-ray and ex situ neutron diffraction to help shed further light on structural phenomena in the >4 V range. $Li_xMn_2O_4$ samples were extracted from charged half-cells and their structures refined by the Rietveld method. At ca. 4.1 V, a spinel-phase of composition $Li_{0.74}Mn_2O_4$ corresponds to a distinct step in the charging curve, suggestibly related to a Mn^{3+} (high-spin) to Mn^{4+} (low-spin) transition. The refined composition for the λ-MnO_2 phase at 4.3 V was $Li_{0.28}Mn_2O_4$, and showed no evidence of lithium/hydrogen ion-exchange. Electrochemical delithiation to form the λ-MnO_2 phase is concluded to involve a single spinel phase and not a coexistence of two-phases.

Keywords: Lithium-ion batteries; Electrochemical delithiation; Spinel; Neutron diffraction

1. Introduction

Lithium manganese oxides are currently amongst the most attractive cathode materials for rechargeable lithium-ion and lithium-ion polymer batteries [1–3], since they have clear strategic advantages over $LiCoO_2$ and $LiNiO_2$ [4] by virtue of their high specific capacity, in combination with low manufacturing cost, long cycle-life and superior environmental advantages. Attention has been directed particularly towards the cubic spinel $LiMn_2O_4$ (space group: *Fd3m*) [5–8], in which oxygen atoms (32*e* sites) coordinate octahedrally around Mn (16*d* sites) and tetrahedrally around Li (8*a* sites). This Mn–O arrangement constitutes the three-dimensional host framework for the redox processes related to the successive extraction and insertion of lithium ions in an electrochemical cell: lithium extraction from the 8*a* site begins at ca. 4.0 V vs. Li/Li^+, and continues until extraction is complete at 4.3 V and we are left with λ-MnO_2. It can be noted that the cubic spinel structure is maintained over the entire composition range $Li_{1-x}Mn_2O_4$, $0 \leq x \leq 1$.

A problematical feature which is often claimed to limit the more widespread use of $LiMn_2O_4$ as a positive electrode, however, is capacity-fade on cycling. This can be attributed to a number of factors:

- Oxidation of the organic-based electrolyte at the high-voltage end of the cycle.

*Corresponding author.
E-mail address: helena.berg@kemi.uu.se (H. Berg)

0167-2738/99/$ – see front matter
PII: S0167-2738(99)00235-0

- Slow dissolution of Mn^{2+} ions into the electrolyte through to the disproportionation reaction: $2Mn^{3+} \rightarrow Mn^{4+} + Mn^{2+}$.
- Retention of lithium atoms in the structure after the first charge/discharge cycle.

Considering each of these in turn: (i) An EC/DMC-based electrolyte has been reported to be both stable with respect to $LiMn_2O_4$ and resistant to oxidation up to 4.8 V [9]; (ii) Several research groups have reported improved performance through suppression of Mn^{3+} disproportionation by substitution of the manganese sites ($Li_xM_yMn_{2-y}O_4$); typically, the effect of substitution by cobalt has been reported in Ref. [10]. In this paper, we focus on the third factor, the retention of lithium. We do this by charging electrochemical cells to a series of voltages above 4 V and thereafter dismantling them and removing the partially delithiated $Li_xMn_2O_4$ material and subjecting it to structural analysis by ex situ neutron powder diffraction. The $Li_xMn_2O_4$ compositions of particular interest occur in the 'single-phase' (quasi-vertical) regions of the discharge curve, i.e. at ca. 4.1 and 4.5 V vs. Li/Li^+ (A and B in Fig. 1). Such neutron diffraction studies should reveal evidence of any lithium/hydrogen ion-exchange, as in the case of chemically delithiated $LiMn_2O_4$ [11]. Definitive information relating to the proposed region of two-phase coexistence between 4.1 and 4.5 V should also be attainable [12–14].

2. Experimental

2.1. Sample preparation and characterisation of spinel powder

$LiMn_2O_4$ powder was prepared by reacting Li_2CO_3 and MnO_2 together in a 1:2 Li:Mn ratio. The mixture was ball-milled and heated slowly (<3°C/min) to 725°C, and calcined in air for 12 h. On cooling to 400°C, the sample was stirred and calcined once more. The temperature was then raised to 725°C (at <1.5°C/min), where it was held for 18 h, and then slowly decreased to room temperature (at <1°C/min). Phase identification was performed at room-temperature by X-ray diffraction using a STOE & CIE GmbH STADI position-sensitive detector (PSD) diffractometer with strictly monochromatic $CuK\alpha_1$-radiation in the 2θ range 10.0–90.0°.

2.2. Cell preparation

Spinel powder (80 wt%) was mixed with 15 wt% carbon black and 5% EPDM (ethylene propylene

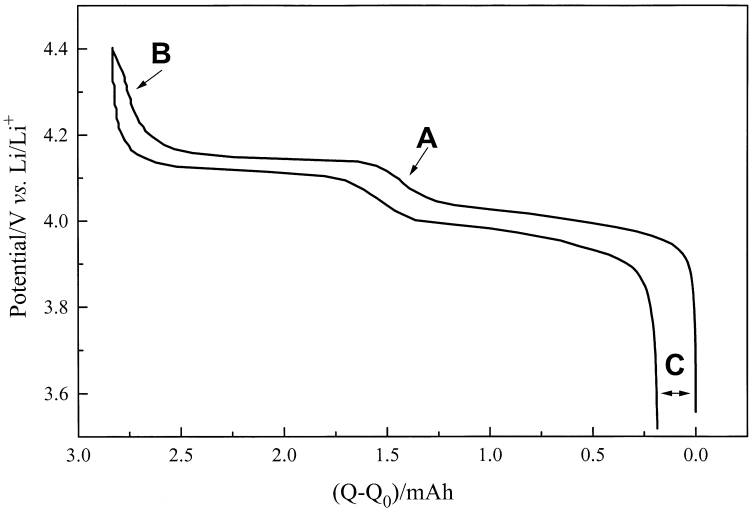

Fig. 1. The first-cycle charge/discharge curve for $LiMn_2O_4$. A and B are the phases studied by ex situ neutron diffraction; C corresponds to the capacity loss during the first cycle.

diene terpolymer) rubber binder, and dissolved in cyclohexane. The slurry was ball-milled for 1 h, spread onto an aluminium foil, and the cyclohexane allowed to evaporated at elevated temperature (80°C) in air. The active cathode thickness was ca. 65 μm.

The cells were assembled in a glovebox under a dry argon atmosphere (<1 ppm H_2O/O_2). The counter electrode was lithium foil, and the electrolyte was a 1 M solution of $LiBF_4$ in 2:1 EC:DMC. The complete laminate comprising the cathode, a separator (Solupor) soaked in the electrolyte, and the lithium-foil anode was vacuum-sealed in an aluminised polymer (Lamofoil™) pouch. Anode and cathode current-collector tabs of nickel and aluminium foils, respectively, passed through the vacuum seal. Appropriate electrode sizes were: 6.6 cm^2 discs for transmission in situ X-ray diffraction, and larger ca. 185 cm^2 rectangular electrodes for ex situ neutron diffraction.

2.3. Ex situ neutron diffraction

The large-area cells intended for ex situ neutron diffraction had OCV's of ca. 3.5 V vs. Li/Li^+. Cells were connected three-by-three to the MacPileII™ system, and charged at room temperature in potentiostatic mode (steps of 0.01 V) to two target voltages: 4.10 and 4.50 V, respectively (the quasi-vertical regions in the charge curve). The potential was incremented when the current fell below 0.01 mA/cm^2. When the desired potentials were reached, the cells were disconnected and left to relax; they reached constant OCV's of 4.096 and 4.304 V, respectively. The cells were dismantled in an argon-filled glovebox (<2 ppm H_2O/O_2); the cathode materials were then scraped carefully from the aluminium current-collectors and sealed into vanadium tubes.

Neutron diffraction data were collected at the steady-state medium-flux research reactor R2 in Studsvik, Sweden. A monochromator system with two copper crystals (220-reflection) were used in parallel alignment ($\lambda = 1.47$ Å). Diffractograms were collected at room temperature (295 K) in the 2θ range 4.00–139.92° in steps of 0.08°. Data were also collected on the initial $LiMn_2O_4$ powder under the same conditions.

2.4. Structure refinement of neutron diffraction data

Structure refinements of the $LiMn_2O_4$ and $Li_xMn_2O_4$ samples were based on the Rietveld method using the program FULLPROF [15,16]. The powder diffraction profile used in the refinement covered the 2θ range 15–135°. Neutron scattering lengths used were Li: -1.90, Mn: -3.73 and O: 5.803 fm. The diffraction peaks were described by a pseudo-Voigt function; a Lorentzian contribution to the Gaussian peak-shape was also refined. Peak asymmetry corrections were made for angles below 45° in 2θ. Absorption was corrected using the experimentally determined μR-value of 0.24. Background intensities were described in different ways: for the pure spinel sample, a polynomial expression $y_i = \Sigma\, B_m((2\theta_i/90) - 1)^m$ was used, where $0 \le m \le 5$; the B_m coefficients for $m = 0$, 1, 2, 3 and 4 were refined together with a scale factor and a 2θ zero-point parameter. In the refinements of the data from the two delithiated spinel samples, the background was described by a linear interpolation between ca. 20 background points on the profile. A lattice parameter and an atomic positional parameter for oxygen were refined for the cubic phase. The lithium content was also refined for the delithiated samples. Since occupancies and displacement parameters are highly correlated, isotropic displacement parameters for each crystallographic site were fixed in the refinements of the delithiated phases to the values obtained from the refinement of the pure spinel sample.

2.5. In situ X-ray diffraction

The cell was placed in the in situ XRD device [17] and fitted to a STOE & CIE GmbH STADI position-sensitive detector (PSD) diffractometer with strictly monochromatic Cu$K\alpha_1$-radiation. As prepared, the open-circuit voltage (OCV) of the cell was 3.19 V; which was then charged in potentiostatic mode using a MacPileII™ cycling system. The potential was raised in steps of 0.1 V to 4.0 V, and from 4.0 V to 4.5 V in steps of 0.05 V. The potential was incremented when the current fell below 0.5 $\mu A/cm^2$ to ensure that a close to equilibrium condition was reached. After 4.5 V vs. Li/Li^+, the cell was

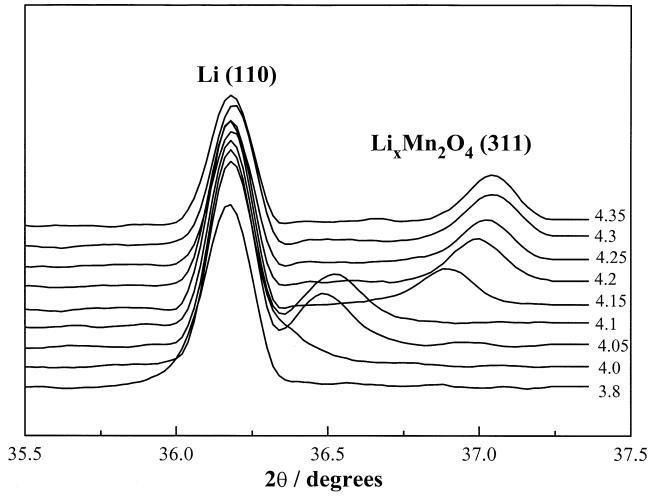

Fig. 2. Profiles obtained from in situ X-ray diffraction during the first charge cycle.

discharged under the same conditions. Diffraction data were collected in transmission mode in the limited 2θ range 34.5–37.5° at each potential; the range contained a metallic lithium (110) monitor reflection and the (113) reflection from $LiMn_2O_4$: see Fig. 2.

3. Results and discussion

3.1. Changes in lattice parameter

X-ray diffraction could verify that the starting material was indeed phase-pure cubic $LiMn_2O_4$. The neutron powder diffraction data could be refined in the cubic space group *Fd3m*, and the parameters obtained from the Rietveld refinement are given in Table 1.

When lithium ions are extracted from $LiMn_2O_4$, the lattice parameter decreases. This process has been studied using in situ X-ray diffraction. Fig. 3 shows the change in lattice parameter as a function of cell potential. At potentials above 4.20 V, the lattice parameter levels off as the λ-MnO_2 phase is reached. The value of the lattice parameter for the λ-MnO_2 phase obtained from the in situ X-ray diffraction ($a=8.037(2)$ Å) agrees well with that obtained by Ohzuku et al. [18] ($a=8.033$ Å). Fig. 4

Table 1
A summary of the refinement of ex situ neutron diffraction data for different electrochemically delithiated $Li_xMn_2O_4$ phases

Potential (V) vs. Li/Li^+	(start material)	4.1	4.3
x in $Li_xMn_2O_4$ (8*a* site)	1.0	0.74(5)	0.28(5)
No. of reflections	45	45	41
No. of refined parameters	16	9	9
No. of background points	Polynom.	24	20
Lattice parameter (a/Å)	8.2211(4)	8.144(2)	8.043(1)
Oxygen coordinate (x_O)	0.2632(1)	0.2624(4)	0.2624(4)
Temp. factor (B/Å^2): Li	1.38(19)	*	*
Mn	0.52(5)	*	*
O	1.15(3)	*	*
R_p(%)	4.51	1.46	1.60
R_{wp}(%)	5.86	1.46	1.60
χ^2	1.63	1.33	1.83

* Value fixed to that obtained from the refinement of the starting material.

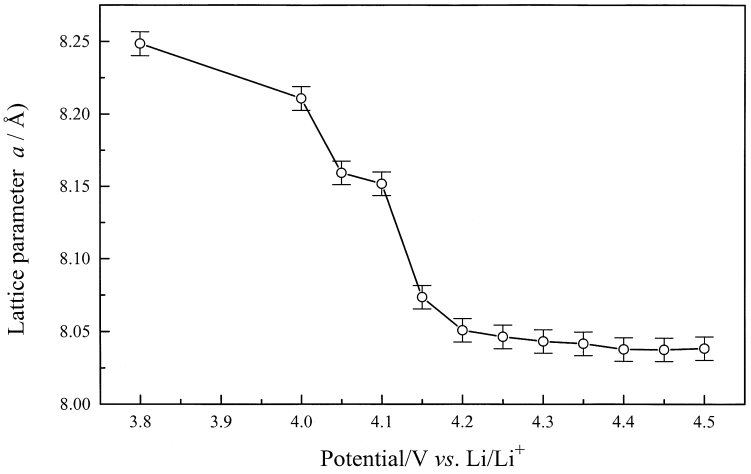

Fig. 3. The spinel lattice parameter (a) plotted as a function of cell potential.

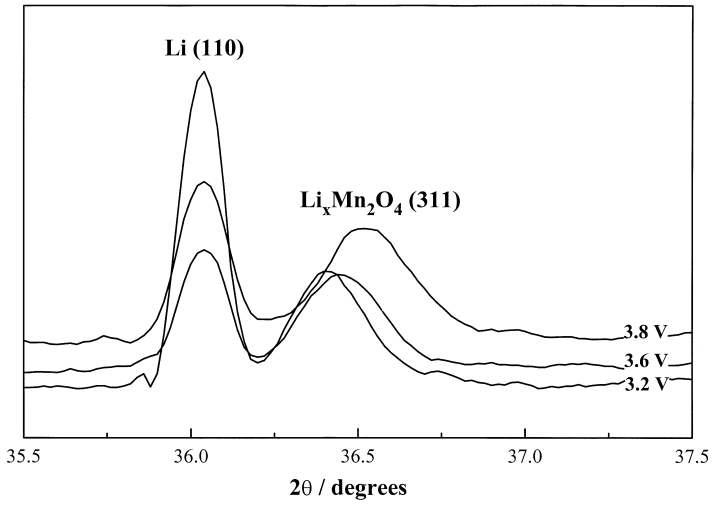

Fig. 4. Profiles obtained from in situ X-ray diffraction during the first discharge cycle.

shows a selected range in the X-ray diffraction profiles measured during the discharge process of the cell. The (113) reflection for the $Li_xMn_2O_4$ phase remains separated from the (110) reflection of metallic lithium. Some lithium is lost during the first charging cycle of the cell, so that $Li_{x=1}Mn_2O_4$ is never reached during the first discharge, with a resulting loss in capacity (C in Fig. 1).

3.2. The delithiated structures

It is clear from the in situ X-ray diffraction studies that the Mn–O framework remains intact during delithiation; the peak positions are merely shifted and no additional peaks are observed. The only changes are the lithium occupations and the oxygen coordinate (*x*, *x*, *x*). Lithium was found only at the 8*a*

site; the same site as in the $LiMn_2O_4$ start material. The in situ X-ray diffraction study shows that the lattice parameter is almost constant (8.037 Å) at potentials above 4.25 V (Fig. 3); a value corresponding to the λ-MnO_2 phase.

Incoherent neutron scattering, originating from the hydrogen atoms in the electrolyte and binder, gives rise to a high background. However, the Bragg reflections from $Li_xMn_2O_4$ are nonetheless observed significantly and the data can be refined satisfactorily (Figs. 5a and 5b). The resulting refined parameters for the two electrochemically delithiated spinels are summarised in Table 1.

It is found that lithium remains in the 8*a* site of electrochemically delithiated λ-MnO_2 to the extent of 0.28 Li per two Mn. This λ-MnO_2 phase can also be obtained by chemical delithiation of $LiMn_2O_4$. According to Hunter [19], chemically delithiated λ-MnO_2 contains only ca. 0.1 Li per two Mn; suggesting that a strong oxidising agent is needed to

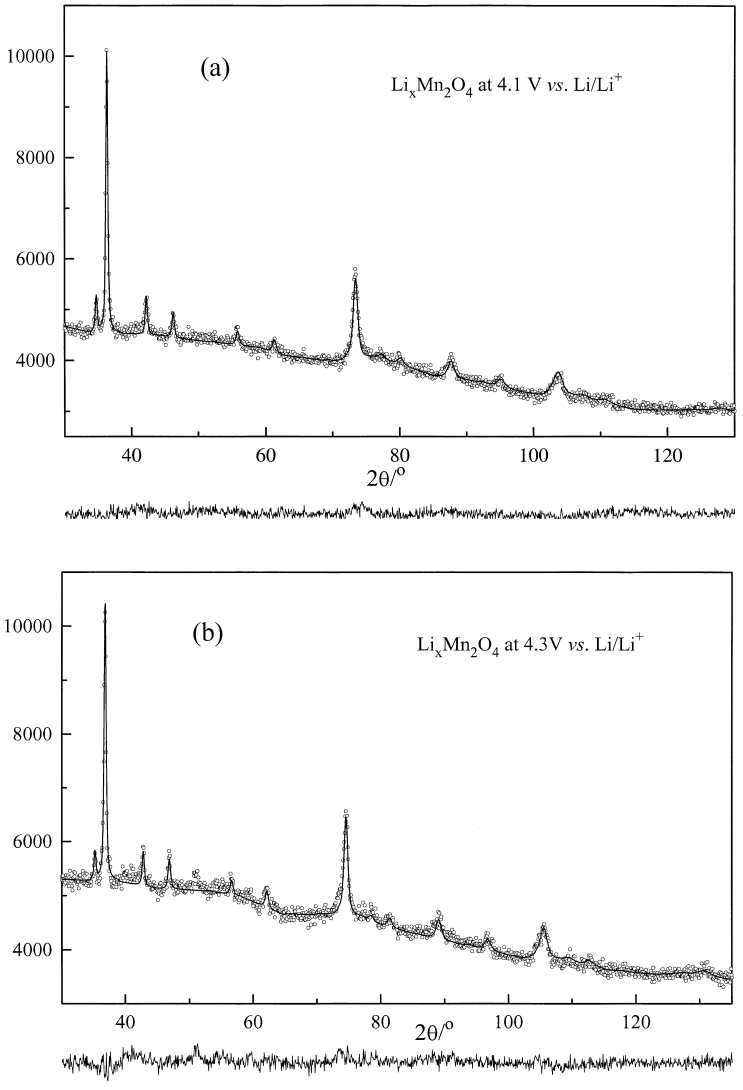

Fig. 5. Rietveld fits of neutron powder diffraction data with background not subtracted for $Li_xMn_2O_4$ at: (a) 4.1 V and (b) 4.3 V vs. Li/Li^+. Differences between refined and calculated profiles are given below each figure.

extract more lithium. Moreover, it has been shown that there is also an ion exchange between Li and H during the acid treatment to obtain the λ-MnO_2 phase [11]; the hydrogen atoms were refined at 96*g* sites ca. 1.1 Å from oxygen atoms. In this present work, difference Fourier syntheses were used to ascertain whether lithium/hydrogen exchange had occurred on charging the cell. No hydrogen atoms could be refined ca. 1 Å away from oxygen atoms in either of the delithiated phases. This is consistent with the apparent stability of the electrolyte, and the fact that no gas evolution was observed throughout the very slow charging process.

3.3. Structural changes

A $Li_{0.5}Mn_2O_4$ phase has been proposed to correspond to the small step in the discharge curve at ca. 4.1 V; e.g. [12]. This composition was calculated assuming that all current passed can be related to lithium-ion insertion/extraction, and that all lithium atoms can be totally removed from the spinel structure. Composition has been refined here from neutron diffraction data to $Li_{0.74}Mn_2O_4$, with a lattice parameter of 8.144(2) Å. It is quite clear that current passed through the cell corresponds not only to lithium-ion insertion/extraction processes. Other electrochemical processes occur in the cell; typically, the formation of some form of oxidised electrolyte-layer on the $LiMn_2O_4$ cathode [20].

Earlier work [21,22] has proposed an ordering of lithium atoms to explain the double plateaus in the charge–discharge curves of $LiMn_2O_4$. However, Liu et al. can only conclude a random ordering of the lithium atoms [12], and suggest that the 'single-phase' region at ca. 4.1 V vs. Li/Li^+ must have some other explanation than the lithium ordering in the structure. It could be that the step in potential observed here for the composition $Li_{0.74}Mn_2O_4$ is a consequence of a change in oxidation state for some of the Mn ions. Using simplistic arguments, from a starting situation involving equal numbers of Mn^{3+} and Mn^{4+} ions, it would require that one Mn^{3+} ion in four becomes oxidised to Mn^{4+}. This could correspond to some form of short-range-ordering (SRO) process involving the formation of a superlattice; e.g a $2\times2\times1$ cell. This could occur without having a noticeable effect on the diffraction pattern. It would be logical to suggest this same type of ordering process in the electrochemically obtained λ-MnO_2 phase, whereby only one Mn^{3+} ion in four remains unoxidised to Mn^{4+}.

Such structural subtleties require, however, the use of more careful techniques for their resolution, typically single-crystal X-ray diffraction.

4. Conclusions

Electrochemical and crystallographic data combine to show that the λ-MnO_2 phase is formed at potentials above ca. 4.25 V vs. Li/Li^+. The refined composition of the electrochemically obtained λ-MnO_2 phase was $Li_{0.28}Mn_2O_4$. This large amount of remnant lithium in the spinel structure is a clear source of capacity loss during the first charge/discharge cycle. These lithiums occupy the tetrahedral 8*a* site, and can only be removed using some strong oxidation agents such as a strong acid. It has also been shown that no lithium/hydrogen ion-exchange occurs during the first cycle. The discharge curve has a single-phase region at ca. 4.1 V vs. Li/Li^+, corresponding to a composition $Li_{0.74}Mn_2O_4$. Why this composition coincides with a step in the discharge curve is not clearly understood. At this composition the oxidation state of Mn increases, and would correspond to 3/8 Mn^{3+} and 5/8 Mn^{4+}.

Acknowledgements

This work has been supported by grants from The Swedish Natural Science Research Council (NFR), The Swedish Board for Technical Development (NUTEK) and EEC (Joule III). All are hereby gratefully acknowledged. We are also indebted to H. Rundlöf for his skilled assistance during the neutron data collection, and to H. Björk for her help during cell preparation.

References

[1] M.M. Thackeray, W.I.F. David, P.G. Bruce, J.B. Goodenough, Mat. Res. Bull. 18 (1983) 461.

[2] I.J. Davidson, R.S. McMillan, J.J. Murray, J.E. Greedan, J. Power Sources 54 (1995) 232.
[3] A.R. Armstrong, P.G. Bruce, Nature (London) 381 (1996) 499.
[4] K. Mizushima, P.C. Johns, P.J. Wiseman, J.B. Goodenough, Mat. Res. Bull. 15 (1980) 783.
[5] M.M. Thackeray, A. de Kock, M.H. Rossouw, D. Liles, R. Bittihn, D. Hoge, Electrochem. Soc. 139 (1992) 363.
[6] J.M. Tarascon, W.R. McKinnon, F. Coowar, T.N. Bowner, G. Amatucci, D. Guyomard, J Electrochem. Soc. 141 (1994) 1421.
[7] R. Koksbang, J. Barker, M.Y. Saïdi, K. West, B. Zachau-Christiansen, S. Skaarup, Solid State Ionics 83 (1996) 151.
[8] G. Pistoia, D. Zane, Y. Zhang, J. Electrochem. Soc. 142 (1995) 2551.
[9] D.G. Guyomard and J.M. Tarascon, US Patent No. 5 192 629 (1993).
[10] R. Bittihn, R. Herr, D. Hoge, J. Power Sources 43–44 (1993) 223.
[11] B. Ammundsen, D.J. Jones, J. Rozière, H. Berg, R. Tellgren, J.O. Thomas, Chem. Mater. 10 (1998) 1680.
[12] W. Liu, K. Kowal, G.C. Farrington, J. Electrochem. Soc. 145 (1998) 459.
[13] S. Mukerjee, T.R. Thurston, N.M. Jisrawi, X.Q. Yang, J. McBreen, M.L. Daroux, J. Electrochem. Soc. 145 (1998) 466.
[14] X.Q. Yang, X. Sun, S.J. Lee, J. McBreen, S. Mukerjee, M.L. Daroux, Electrochem. Solid-State Lett. 2 (1999) 157.
[15] H.M. Rietveld, J. Appl. Cryst. 2 (1969) 65.
[16] J. Rodriguez-Carvajal, ILL Internal Report, FULLPROF computer program.
[17] Ö. Bergström, T. Gustafsson, J.O. Thomas, J. Appl. Cryst. 31 (1998) 103.
[18] T. Ohzuku, M. Kitagawa, T. Hirai, J. Electrochem. Soc. 137 (1990) 769.
[19] J.C. Hunter, J. Solid State Chem. 39 (1981) 142.
[20] T. Eriksson, T. Gustafsson, J.O. Thomas, Proc. Electrochem. Soc. 98 (16) (1999) 315.
[21] W. Liu, G.C. Farrington, F. Chaput, B. Dunn, Electrochem. Soc. 143 (1996) 879.
[22] R.J. Gummow, M.M. Thackeray, J. Electrochem. Soc. 141 (1994) 1178.